



## CAA-based acoustic beamforming for noise identification in complex media

Vincent Fleury, Daniel Mincu, Cyril Polacsek

### ► To cite this version:

Vincent Fleury, Daniel Mincu, Cyril Polacsek. CAA-based acoustic beamforming for noise identification in complex media. Acoustics 2012, Apr 2012, Nantes, France. hal-00811126

HAL Id: hal-00811126

<https://hal.science/hal-00811126>

Submitted on 23 Apr 2012

**HAL** is a multi-disciplinary open access archive for the deposit and dissemination of scientific research documents, whether they are published or not. The documents may come from teaching and research institutions in France or abroad, or from public or private research centers.

L'archive ouverte pluridisciplinaire **HAL**, est destinée au dépôt et à la diffusion de documents scientifiques de niveau recherche, publiés ou non, émanant des établissements d'enseignement et de recherche français ou étrangers, des laboratoires publics ou privés.



Distributed under a Creative Commons Attribution 4.0 International License



# ACOUSTICS 2012

## CAA-based acoustic beamforming for noise identification in complex media

Y. Pene<sup>a</sup>, V. Fleury<sup>a</sup>, D. C. Mincu<sup>a</sup> and C. Polacsek<sup>b</sup>

<sup>a</sup>ONERA, 29 avenue de la Division Leclerc, 92322 Chatillon, France

<sup>b</sup>Onera, Département de Simulation Numérique des Ecoulements et Aéroacoustique, BP 72 -  
29, avenue de la Division Leclerc, 92322 Chatillon Cedex  
[yves.pene@onera.fr](mailto:yves.pene@onera.fr)

Beamforming methods use analytical Green functions to describe the acoustic propagation between noise sources and microphones. For example, due to flow heterogeneity and complex boundary conditions, the Green functions become analytically difficult to determine in the case of a realistic turbofan engine. The aim of this work is to overcome the analytical Green functions determination difficulties by employing CAA tools. In order to numerically evaluate these functions, we propose a method based on non linear euler equations implemented in the Onera's sAbraInA-v0 code. The noise source area is sampled as a finite distribution of monopoles which emit simultaneously. The sound field is then computed from the source points to the microphones. An ARMA based algorithm is applied to evaluate Green functions between each monopole and each microphone. First of all, the approach is validated from analytical simple test cases, such as the propagation of a monopole in uniform flow. Once achieved, more delicate problems will be processed, such as the presence of multiple sources, flow gradients and complex geometries.

## 1 Introduction

In the last thirty years, beamforming techniques have become a common tool to identify the noise sources and characterize the acoustic levels for both academic and industrial problems. Beamforming techniques are based on knowledge of a propagation model, between sources and microphones, *i.e.* the Green's function. This function is generally known for simple cases such as the radiation in the free and uniform flow, annular duct propagation or rectangular reverberation rooms [1]. To take into account an infinite thin shear layer, Amiet [2] proposed an improved method, largely used since (Humphreys [3], Padois [4]) in experimental measurements treatment. But in realistic industrial problems, the propagation medium properties are largely more complex. In such cases, not using an appropriate Green's function can lead to spurious sources localization and may create a bias of level estimation. The purpose of this paper is to overcome this limitation and implicitly to improve the analysis of experimental data by using CAA as an estimator of Green's function. To perform CAA computations we chose the Onera's sAbraInA-v0 code which solves the Euler equations in perturbation form using high order spatial and temporal schemes. The benefit of this method is represented by the possibility to compute the acoustical propagation over complex flows and realistic geometries [6]. In this paper we focus on the validation of Green's function estimation by using CAA. In such a way, the method is verified on known solutions, such as one or more monopoles propagation in uniform flows or in the presence of infinite rigid walls.

## 2 Problem formulation

Let's consider  $M$  broadband source points and a set of  $N$  microphones within a propagation medium (see Figure 1). The purpose is to determine the Green's function  $G_{m,n}(\omega)$  between each source point  $m$  and each microphone  $n$ , *via* the sAbraInA-v0 solver. A first possible approach is to separately simulate the acoustical emission of each source to the microphones. However, this involves a prohibitive number of simulations, equal to the number  $M$  of source points. In order to overcome this drawback, we propose to simulate the acoustic emission of all the sources points simultaneously. The task is then to separate the contribution of each source on global emission in order to get  $G_{m,n}(\omega)$ . The procedure is presented in the following section.

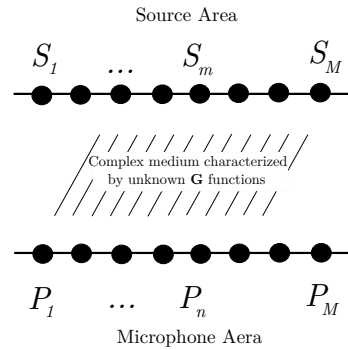


FIGURE 1 – Schematization of the problem, discretization of the source and listening area.

## 3 Methodology

The Fourier transform  $P_n(\omega)$  of the microphone signal  $n$  is related to the Fourier transform of every source signals  $S_m(\omega)$  by the following equation

$$P_n(\omega) = [G_{1,n}(\omega) \dots G_{M,n}(\omega)] [S_1(\omega) \dots S_M(\omega)]^+ \quad (1)$$

where  $+$  represents the non-conjugate transpose. This system is highly underdetermined. A frequency domain model is therefore introduced for  $G_{m,n}(\omega)$ ,

$$\hat{G}_{m,n}(\omega) = \sum_{l=0}^L b_{m,n}(l) \exp(j\omega l T_e), \quad (2)$$

where  $T_e$  represents the time sampling used to compute the Fourier transforms  $P_n(\omega)$  and  $S_m(\omega)$ . The unknown  $b_{m,n}(l)$  coefficients are determined by minimizing the following equation for every  $n$

$$\epsilon_n = \sum_{\omega=\omega_{\min}}^{\omega_{\max}} \left| P_n(\omega) - \sum_{m=1}^M S_m(\omega) \sum_{l=0}^L b_{m,n}(l) \exp(j\omega l T_e) \right|^2 \quad (3)$$

The parameters  $\omega_{\min}$  and  $\omega_{\max}$  are determined from computational criteria. This is explained in Sec. 4.1. In Eq. (3), the summation over the frequency range  $[\omega_{\min}, \omega_{\max}]$  enables to provide supplementary constraints with respect to Eq. (1). The number of parameters to be determined is  $N_p = LM$  and the number of constraints is  $N_c = (\omega_{\max} - \omega_{\min})/\Delta f$ , where  $\Delta f$  is the frequency resolution of the Fourier transform. In order to get a well-posed minimization problem Eq. (3),  $L$  is chosen such as  $N_p \leq N_c$ . Finally, the solution is computed using a straightforward pseudo-inverse procedure.

## 4 Numerical applications for 2D test cases

Different test cases are considered :

- one single source, one microphone, free field medium,
- two sources, one microphone, free field medium,
- two sources, one microphone, uniform flow medium,
- two sources, one microphone, uniform flow medium, infinite reflecting wall.

The main interest of these test cases is that an analytical formulation of the Green's function is available for comparison.

### 4.1 Simulation parameters

For the sake of reasonable computational time a reduced 2D problem is considered and a limited frequency domain is simulated. We choose a 100-by-100 cells cartesian grid and  $\omega_{\min} = 1500$  Hz and  $\omega_{\max} = 3000$  Hz. In order to accurately compute the acoustic signal up to  $\omega_{\max}$  (ten grid points per  $\lambda_{\min}$ ) a spatial step  $\Delta x = 0.01$  m is taken. To ensure a non reflecting boundary condition down to  $\omega_{\min}$ , a smooth grid stretching is necessary up to two grid points per  $\lambda_{\max}$  outer the  $\Delta x$  consistant zone. To get a CFL number around 0.6, the time sampling used is  $\Delta t = 20 \mu\text{s}$ . Each source is described as follows,

$$s(\vec{y}, t) = h(\vec{y})f(t) \quad (4)$$

Theoretically, to compute the Green's function,  $h(\vec{y})$  should be considered as a Dirac distribution. However, to preserve the computational stability an extended spatial source is used. A Gaussian source distribution is chosen

$$h(\vec{y}) = \frac{1}{\kappa^2} \exp\left(-\pi \frac{|\vec{y} - \vec{y}_0|^2}{\kappa^2}\right), \quad (5)$$

where  $\vec{y}_0$  is the center of the source. In order to ensure the compacity of the source, the  $\kappa$  parameter is chosen sufficiently small with the respect to  $\lambda_{\min}$  ( $\lambda_{\min} = 2\pi/\omega_{\max}$ ). The optimal  $\kappa$  value is found to be  $\kappa = 0.3\lambda_{\min}$ . This is justified in the following.

Concerning  $f(t)$  in Eq. (4), it should also be considered as a Dirac distribution. But we limit the emission frequency range from  $\omega_{\min}$  to  $\omega_{\max}$ , by using a filtered broadband signal.

Generally, for the tested cases the convergence of the CAA computation is reached after  $300 \Delta t$  and  $5000 \Delta t$  are supplementary performed in order to get a frequency resolution of  $\Delta f = 10$  Hz. The total computational duration is of about 10 minutes for the numerical Green's function estimation with a conventional computer.

### 4.2 Single source in free field, without flow

A single source ( $M = 1$ ) is considered in free-field in  $(y_1 = 0, y_2 = 0)$  and a single microphone ( $N = 1$ ) is placed in  $(x_1 = 0.48 \text{ m}, x_2 = 0)$ , see Figure 2. The estimated Green's function  $\hat{G}_{1,1}(\omega)$  is plotted in Figure 3. For comparison, the analytical 2D Green's function is superimposed

$$G_{2D}(\vec{x} - \vec{y}, \omega) = \frac{1}{4i} H_0^1 \left( \frac{\omega}{c} |\vec{x} - \vec{y}| \right) \quad (6)$$

The agreement is deemed satisfying. The slight discrepancy is mainly attributed to the imperfect compacity of the source. Indeed, for an extended noise source as defined in Eqs. (4,5), the emitted acoustic pressure is given by

$$P(\vec{x}, \omega) = F(\omega) \int G_{2D}(\vec{x} - \vec{y}, \omega) h(\vec{y}) d^2 y$$

The resulting frequency-domain Green's function  $P(\vec{x}, \omega)/F(\omega)$  is plotted in Figure 3. The agreement with the estimated Green's function  $\hat{G}_{1,1}(\omega)$  is better, which confirms the influence of compacity effects.

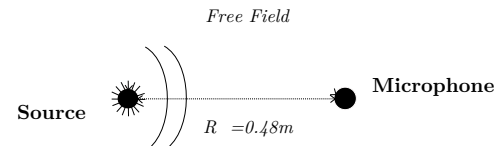


FIGURE 2 – Propagation in free field from one source to a receiver located distance  $R = 0.48$  m.

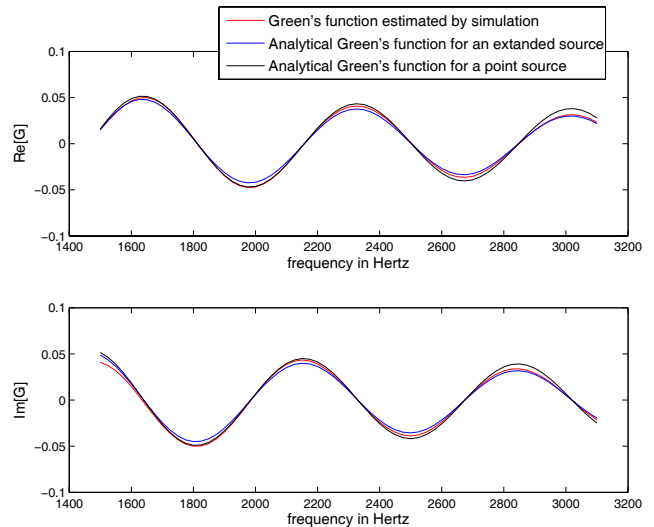


FIGURE 3 – Results obtained for the estimation of the Green's function between a source and a receiver placed at a distance  $R = 0.48$

### 4.3 Case of two monopoles in free field

In the second case, the purpose is to estimate each of the Green's functions in the presence of a receiver and two monopoles simultaneously emitting. As shown in Figure 4, the first source is placed in  $(y_1 = 0.00, y_2 = 0.00)$ , the second in  $(y_1 = 0.00, y_2 = 0.20)$  and the microphone at  $(x_1 = 0.48, x_2 = 0.00)$

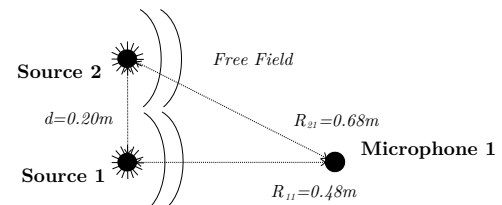


FIGURE 4 – Propagation in free field of two sources to a receiver to the respective distances  $R_{11} = 0.48$  and

$$R_{21} = 0.67$$

The estimated  $\hat{G}_{11}$  and  $\hat{G}_{21}$  functions are respectively presented in Figure 5, and 6 .

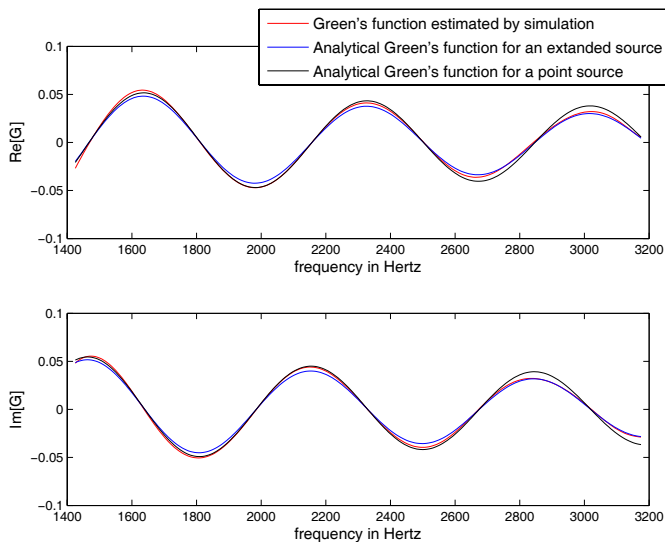


FIGURE 5 – Green’s function  $G_{11}$  between the source  $m = 1$  and receiver  $n = 1$

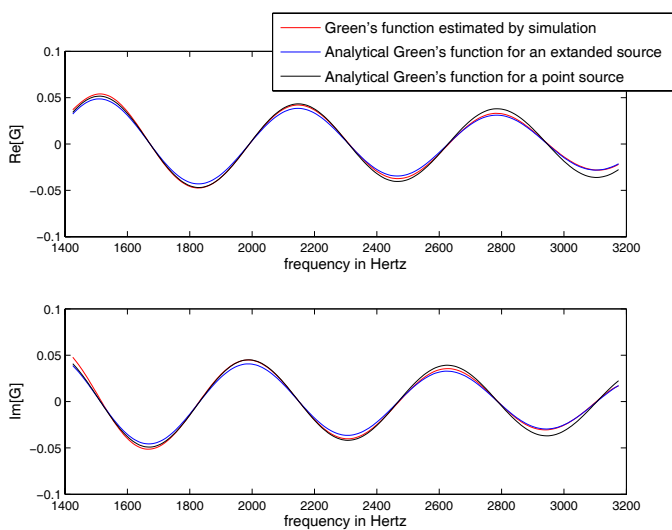


FIGURE 6 – Green’s function  $G_{21}$  between the source  $m = 2$  and receiver  $n = 1$

The results obtained for the two estimated functions show the same agreement as the one obtained for the previous case. We note a slight discrepancy with the Ponctual Green’s function and a good accordance with the Gaussian source Green’s function. In this case, each source contribution has been separated using the estimation model in order to get all the Green’s functions.

#### 4.4 Case of two monopoles in uniform flow

A uniform flow (Mach  $M = 0.2$ ) is introduced into the previous case in the positive direction  $\vec{x}_1$ , see Figure 7. The Green’s function obtained  $G_{11}$  between  $m=1$  and  $n=1$  is plotted in Figure 8 . This results is compared to the analytical 2D Green function  $G_{2Dflow}(\vec{x} - \vec{y}, \omega)$  with uniform flow into the positive direction  $\vec{x}_1$  expressed as follow :

$$G_{2Dflow}(\vec{x} - \vec{y}, \omega) = \frac{1}{4i\beta} H_0^1 \left( k_0 \left( \frac{S_0}{\beta^2} \right) \right) e^{\frac{i k M (x_1 - y_1)}{\beta^2}} \quad (7)$$

with

$$\begin{cases} \beta^2 &= 1 - M^2 \\ S_0^2 &= \beta^2(x_2 - y_2)^2 + (x_1 - y_1)^2 \end{cases} \quad (8)$$

As previously the results is compared with the deduced analytical Green’s function for an extended source given by :

$$H(\vec{x} - \vec{y}, \omega) = P(\vec{x}, \omega) / F(\omega)$$

where

$$P(\vec{x}, \omega) = F(\omega) \int G_{2Dflow}(\vec{x} - \vec{y}, \omega) h(\vec{y}) d^2y$$

The agreement is found satisfying. As above we note a slight better accordance with the extended source Green’s function due to the the influence of compacity effects.

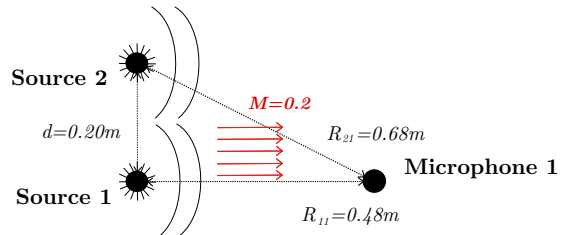


FIGURE 7 – Propagation of two sources in uniform flow  $M = 0.2$  in the direction  $\vec{x}_1$

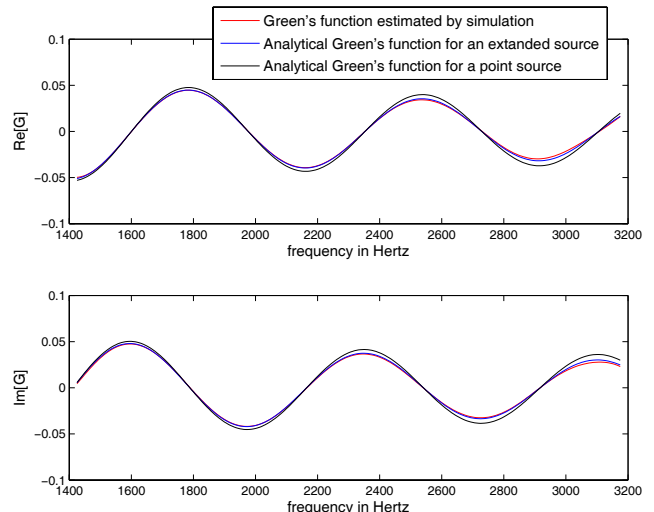


FIGURE 8 – Green’s function  $G_{11}$  between the source  $m = 1$  and the receiver  $n = 1$

## 4.5 Case of two monopoles in uniform flow with an infinite reflector

In this last example, an infinite reflector is added to the previous case as shown schematically in Figure 9.

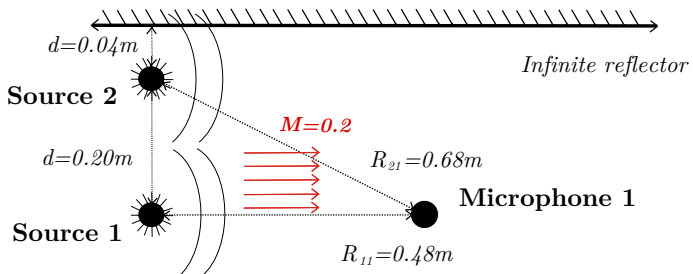


FIGURE 9 – Propagation of two sources in uniform flow  $M = 0.2$  in the direction  $\vec{x}_1$  in the presence of an infinite reflector

The estimated Green's function is plotted in Figure 10. To compare, an analytical Green's function computed by the source-image method is superimposed. More precisely, the source image is considered as the symmetry of the source relative to the reflector. The resulting function is expressed as the sum of the Green's function between the source and receiver, and the one between the source image and receiver :

$$G_{\text{reflector}}(\vec{x} - \vec{y}, \omega) = G(\vec{x} - \vec{y}, \omega) + G(\vec{x} - \vec{y}_{\text{image}}, \omega) \quad (9)$$

As expressed below, the analytical Green function for an extended source is deduced from (9) and superimposed Figure 10.

$$H_{\text{reflector}}(\vec{x} - \vec{y}, \omega) = P(\vec{x}, \omega)/F(\omega)$$

where

$$P(\vec{x}, \omega) = F(\omega) \int G_{\text{reflector}}(\vec{x} - \vec{y}, \omega) h(\vec{y}) d^2y$$

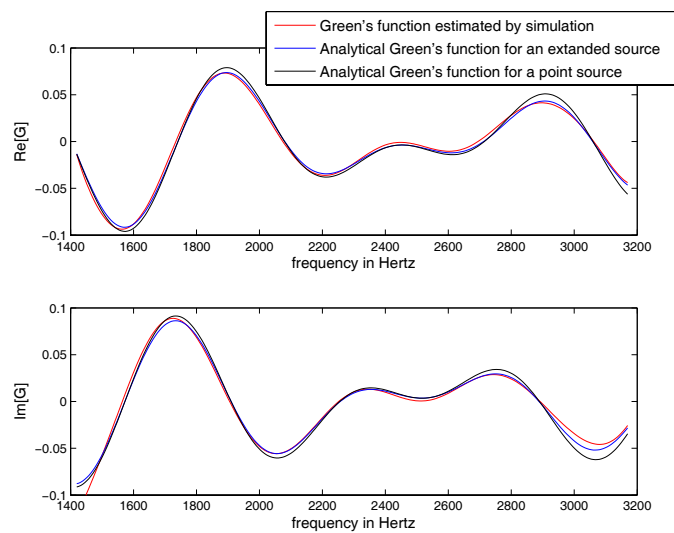


FIGURE 10 – Green's function  $G_{11}$  between the source  $m = 1$  and the receiver  $n = 1$ , in presence of a uniform flow and of a reflector

The obtained results show a good agreement with the analytical Green's function. We note a slight bigger amplitude discrepancy for the point source Green's function than in the previous examples. This test case seems to be more sensitive to the compacity effects.

## 5 Conclusion

The present study aims at assessing new approach to beamforming where the Green's function used is evaluated by CAA to take into account complex propagation effects. In this paper we propose to simulate the acoustic emission of all the sources points simultaneously to the microphones through the complex medium. The results obtained are then processed using a minimization algorithm to estimate the whole Green's function between each point of the plane source and each microphone. To assess the methodology, the results obtained are compared to known solutions, such as one or more monopoles propagation in uniform flows or in the presence of infinite rigid walls. In all proposed tests cases, estimated Green's functions show good agreement with the analytical Green's functions, allowing at first to validate our approach. In subsequent work, the estimated Green's functions will be used to perform simulation of beamforming. We will address in particular the influence of different simulation parameters on the imagery results. The method will be next computed on more complex cases, not known analytically, as well as on real cases from wind tunnel testing.

## Références

- [1] J.B. Allen, D.A. Berkley, "Image method for efficiently simulating small-room acoustics" *J. Acoust. Soc. Am.*, Vol. 65, No.4, April 1979
- [2] R.K. Amiet, "Refraction of sound by a shear layer", *Journal of Sound and Vibration*, 58, 1978
- [3] Jr. W.M. Humphreys, T.F. Brooks, Jr. W.W. Hunter, and K.R. Meadows., "Design and use of microphone directional array for aeroacoustic measurement", *36st Aerospace Sciences Meeting exhibit,AIAA, Reno*, 1998
- [4] T. Padois, C. Prax et V. Valeau "Traitement d'antenne appliqu aux mesures en soufflerie : Prise en compte des effets de l'écoulement sur la propagation au moyen d'un modèle numérique ", *10 Congrès Français d'Acoustique, Lyon*, 2010
- [5] T. Padois, C. Prax et V. Valeau "Potentiality of time-reversed array processing for localizing acoustic sources in flows", *Berlin Beamforming Conference*, 2010
- [6] S. Redonnet, E. Manoha, P. Sagaut,"Numerical simulation of propagation of small perturbations interacting with flows and solid bodies" *7th AIAA/CEAS Aeroacoustics Conference*,Maastricht (2001)
- [7] R.P. Dougherty, B.E. Walker, D.L. Sutliff, "Locating and quantifying broadband fan sources using induct microphones", *16th AIAA/CEAS Aeroacoustics Conference* AIAA Paper 2010-3736.